Original Article

DOI: 10.5582/bst.2025.01065

Exosomes derived from olfactory mucosa mesenchymal stem cells attenuate cognitive impairment in a mouse model of Alzheimer's disease

Xiqi Hu, Ya-nan Ma, Jun Peng, Zijie Wang, Yuchang Liang, Ying Xia*

Department of Neurosurgery, Haikou Affiliated Hospital of Central South University Xiangya School of Medicine, Haikou, China.

SUMMARY: Alzheimer's disease (AD) is a progressive neurodegenerative disorder characterized by cognitive decline, neuroinflammation, and endoplasmic reticulum (ER) stress. In recent years, exosomes have garnered significant attention as a potential therapeutic tool for neurodegenerative diseases. This study, for the first time, investigates the neuroprotective effects of exosomes derived from olfactory mucosa mesenchymal stem cells (OM-MSCs-Exos) in AD and further explore the potential role of low-density lipoprotein receptor-related protein 1 (LRP1) in this process. Using an Aβ1-42-induced AD mouse model, we observed that OM-MSCs-Exos significantly improved cognitive function in behavioral tests, reduced neuroinflammatory responses, alleviated ER stress, and decreased neuronal apoptosis. Further analysis revealed that OM-MSCs-Exos exert neuroprotective effects by modulating the activation of microglia and astrocytes and influencing the ER stress response, a process that may involve LRP1. Although these findings support the potential neuroprotective effects of OM-MSCs-Exos, further studies are required to explore their long-term stability, dose dependency, and immunogenicity to assess their feasibility for clinical applications.

Keywords: cellular stress regulation, microglial activation, astrocytic response, pro-inflammatory cytokines, neuroprotection, cognitive improvement

1. Introduction

With aging of the global population, Alzheimer's disease (AD) has emerged as a major public health challenge and a key focus of neurodegenerative disease research (*1*). The pathological hallmarks of AD primarily include neurofibrillary tangles (NFTs) formed by hyperphosphorylated tau protein and amyloid plaques resulting from the deposition of insoluble β-amyloid protein (Aβ) (*2*). These abnormal proteins progressively accumulate, triggering neuroinflammatory responses, activating microglia and astrocytes, and exacerbating neuronal damage and neurodegenerative changes (*2*).

The pathogenesis of AD is complex, involving multiple cellular and molecular abnormalities, such as endoplasmic reticulum (ER) stress, mitochondrial dysfunction, oxidative stress, and chronic inflammation (*2*). Studies have shown that several ER stress markers, including phosphorylated PERK, phosphorylated IRE1α, phosphorylated eIF2α, XBP1, and CHOP, are significantly upregulated in the brain tissue of patients with AD (*3-5*). Moreover, ER stress enhances γ-secretase activity, promoting Aβ secretion and intensifying the accumulation of abnormal proteins, thereby accelerating the progression of AD (*6,7*).

Despite advances in AD research, the development of effective treatments to slow its progression remains elusive due to its heterogeneity and multifactorial pathogenesis (*8*). Consequently, the development of targeted and innovative therapeutic approaches has become a critical priority in AD research. In recent years, stem cell therapy has gained considerable attention due to its pluripotency and immunomodulatory properties, emerging as a promising avenue in neurodegenerative disease studies (*9,10*). Specifically, research has demonstrated that transplantation of bone marrow-derived mesenchymal stem cells (BMSCs), adipose-derived mesenchymal stem cells (ADMSCs), and neural stem cells (NSCs) can potentially have neuroprotective and reparative effects on neurodegenerative diseases (*8*).

Olfactory mucosa mesenchymal stem cells (OM-MSCs), a unique type of stem cell derived from the ectoderm, retain the immunomodulatory and tissue repair capabilities of traditional mesenchymal stem cells (MSCs) while exhibiting enhanced neurogenic potential. OM-MSCs have displayed distinct advantages in neurodegenerative disease research, particularly due to their minimally invasive isolation from the nasal cavity,

which reduces ethical concerns. Despite the remarkable therapeutic potential of stem cell therapy, however, direct transplantation faces certain limitations, including difficulties in crossing the blood-brain barrier (BBB) and potential tumorigenic risks. As a result, recent studies have increasingly shifted focus toward the paracrine effects of stem cells, and particularly the extracellular vesicles (EVs) and exosomes they secrete.

Exosomes are lipid nanoparticles with diameters ranging from approximately 30 to 150 nanometers, that are capable of carrying a variety of bioactive molecules, such as proteins, nucleic acids, and lipids. Due to their favorable biocompatibility and low immunogenicity, exosomes can effectively cross the BBB, positioning them as an emerging therapeutic strategy for neurodegenerative diseases (*11*). For instance, a study has shown that BMSCs-derived exosomes can significantly ameliorate cognitive dysfunction in AD-like mouse models (*9*).

Nevertheless, the potential role and underlying molecular mechanisms of OM-MSCs-Exos in AD remain largely unexplored. To address this gap, the current study aims to investigate the neuroprotective effects and mechanisms of OM-MSCs-Exos in AD treatment using a mouse model of Aβ1-42-induced AD and an SH-SY5Y cell model. Specifically, this study examines whether OM-MSCs-Exos have an effect by modulating neuroinflammation and ER stress responses. The findings of this study are expected to provide theoretical support for stem cell-based therapeutic strategies in AD and lay the groundwork for future clinical translational research.

2. Materials and Methods

2.1. Isolation and culture of OM-MSCs

Olfactory epithelial tissue was isolated from the nasal cavity of C57BL/6 mice, cut into small pieces, and cultured in DMEM/F-12 medium (Gibco, USA) supplemented with 15% fetal bovine serum (FBS) for 7 days (*12*). Non-adherent cells were removed, and the remaining cells were digested with trypsin and expanded until passage 3.

Surface markers of OM-MSCs were analyzed using flow cytometry. Specifically, 1×10^6 cells (100 μL) were placed in a 1.5 mL EP tube and incubated with antibodies against CD29, CD90, CD44, CD34, CD45, and CD11b (eBioscience, USA). After incubation at room temperature in the dark for 30 minutes, cells were washed with 1 mL PBS and centrifuged at 350 g for 5 minutes. The supernatant was discarded, and the cells were resuspended in 350 μL of PBS for flow cytometry analysis.

Osteogenic and adipogenic differentiation of OM-MSCs was induced under specific culture conditions. For osteogenic differentiation, OM-MSCs were cultured in an osteogenic induction medium (Abiowell, China) for 3 weeks and stained with Alizarin Red to assess differentiation. For adipogenic differentiation, cells were cultured in an adipogenic induction medium (Abiowell, China) for 14 days and stained with Oil Red O to evaluate differentiation.

2.2. Isolation and characterization of OM-MSCs-Exos

OM-MSCs from passages 3–5 were cultured to 90% confluence, washed three times with PBS, and then incubated in medium containing 10% exosome-depleted FBS for 48 hours. The conditioned medium was collected and stored at -80°C.

The collected supernatant was centrifuged at 1500 rpm for 5 minutes, followed by 3000 rpm for 30 minutes to remove cellular debris. The supernatant was then filtered through a 0.22-μm membrane and concentrated *via* ultrafiltration. After centrifugation at 3000 rpm for 10 minutes, exosomes were pelleted by ultracentrifugation at 100,000 g for 2 hours.

The size distribution of exosomes was measured using nanoparticle tracking analysis (NTA, Nanosight NS300, Malvern, UK). The morphology and size of exosomes were observed using transmission electron microscopy (TEM, HITACHI, Japan).

2.3. Animal model and experimental design

Eight-week-old male C57BL/6 mice weighing 23–25 g were purchased from Hunan SJA Laboratory Animal Co., Ltd. All animals met specific pathogen-free standards and were housed under controlled conditions (temperature: 25±1°C; humidity: 60±5%; 12-hour light/dark cycle) with free access to food and water. The experiments were approved by the Ethics Committee of Haikou Hospital Affiliated with Xiangya Medical College, Central South University, and conducted in accordance with the Guide for the Care and Use of Laboratory Animals published by the National Institutes of Health (*13*).

The mouse model of AD was established as previously described (*14*). Mice were randomly divided into five groups: a sham group, an AD group, an AD+OM-MSCs-Exos group, an AD+si-NC-Exos group, and an AD+si-LRP1-Exos group, with 6 mice per group. To induce AD, mice were anesthetized with sodium pentobarbital, and Aβ1-42 (6 μg) was injected bilaterally into the hippocampus (anterior-posterior: -2.0 mm; medial-lateral: ±1.6 mm; dorsal-ventral: 1.5 mm from Bregma) using a stereotaxic apparatus. The control group received an equal volume of saline.

Subsequently, each mouse received tail vein injections of 100 μL PBS, OM-MSCs-Exos, si-NC-Exos, or si-LRP1-Exos (1 mg/mL) twice weekly for 4 weeks. Following the final injection, cognitive function was assessed using the Morris water maze (MWM) test (*15*) and the novel object recognition test (NORT) (*9*).

2.4. Cell experiments

The human neuroblastoma cell line SH-SY5Y (AW-CCH335, Abiowell, China) was cultured in MEM/F-12 medium supplemented with 10% FBS and 1% penicillin/streptomycin at 37°C in a 5% CO_2 incubator. To establish an *in vitro* model of AD, SH-SY5Y cells were treated with 20 μM Aβ1-42 for 24 hours (*15*). For the treatment groups, 40 μg/mL of OM-MSCs-Exos, si-NC-Exos, or si-LRP1-Exos was added to the culture and incubated for 12 hours (*16*).

2.5. TUNEL fluorescence assay

Cell apoptosis was detected using a TUNEL apoptosis detection kit (FITC). Tissue sections were deparaffinized with xylene, dehydrated through a graded ethanol series, and processed using a TUNEL kit (Shanghai Yeasen Biotech, China) according to the manufacturer's instructions. Sections were incubated with 100 μL of proteinase K working solution at 37°C for 20 minutes, followed by 100 μL 1× equilibration buffer at room temperature for 10–30 minutes. Subsequently, 50 μL of TdT incubation buffer was added, and sections were incubated at 37°C in the dark for 60 minutes. Nuclei were stained with DAPI working solution at 37°C in the dark for 10 minutes. After mounting, sections were observed under a fluorescence microscope.

2.6. Nissl staining

Tissue sections were deparaffinized with xylene and dehydrated through a graded ethanol series before Nissl staining. Differentiation was performed using a specific differentiation solution. Sections were mounted with glycerol and observed under a microscope.

2.7. Immunohistochemistry (IHC)

Brain tissue was dehydrated through a graded ethanol series, embedded in paraffin, and sectioned. Sections were deparaffinized, rehydrated, and subjected to antigen retrieval by heating. They were then incubated at 4°C with primary antibodies against GFAP (PTG, USA) and IBA1 (Abiowell, China) overnight. After they were washed three times with PBS, sections were incubated with HRP-conjugated secondary antibodies. Color development was achieved using a DAB substrate, followed by counterstaining with hematoxylin. Sections were subsequently observed under a microscope.

2.8. RT-qPCR

Total RNA was extracted using a Trizol reagent (Thermo, USA) and reverse-transcribed into cDNA. RT-qPCR was performed using the UltraSYBR Mixture (Beijing CWBio, China). Primers were synthesized by Beijing Tsingke Biotech Co., Ltd. The RT-qPCR protocol included denaturation at 95°C for 10 minutes, followed by 40 amplification cycles (95°C for 15 seconds, 60°C for 30 seconds) (Supplemental Table S1, *https://www.biosciencetrends.com/action/getSupplementalData.php?ID=248*),

2.9. ELISA

Levels of IL-1β, IL-6, TNF-α, and Aβ1-42 expression in brain tissue and cell culture supernatant were measured using ELISA kits (Wuhan Fine Biotech, China) according to the protocol provided.

2.10. Western blot (WB)

Protein concentrations were quantified using a BCA protein assay kit (Abiowell, China). Equal amounts of protein were loaded onto SDS-PAGE gels and transferred to PVDF membranes for immunoblotting. Primary antibodies included Calnexin (Abiowell, China), CD9 (Abiowell, China), CD63 (Proteintech, USA), BCL-2 (Abiowell, China), BAX (Abiowell, China), Cleaved-caspase3 (PTG, USA), CHOP (Abiowell, China), GRP78 (Abiowell, China), ATF6 (Abcam, UK), LRP1 (Abcam, UK), and β-actin (Abiowell, China). Membranes were incubated with primary antibodies at 4°C overnight, followed by HRP-conjugated secondary antibodies. Chemiluminescence was visualized using an ECL detection kit, and band intensities were quantified with the software ImageJ.

2.11. Statistical analysis

Data were analyzed using the software GraphPad Prism 8.0 (GraphPad Software, USA). Normally distributed data are expressed as the mean ± standard deviation, while non-normally distributed data are expressed as the median. Between-group comparisons were evaluated using the Student's *t*-test. For comparisons involving three or more groups, one-way analysis of variance (ANOVA) was used. Qualitative data were analyzed using the chi-square test. A P-value < 0.05 was considered statistically significant.

3. Results

3.1. Isolation and characterization of OM-MSCs and OM-MSCs-Exos

OM-MSCs and OM-MSCs-Exos were successfully isolated and characterized. OM-MSCs were extracted from the olfactory mucosa of mice and passaged to the third generation (P3). Flow cytometry analysis revealed that P3 OM-MSCs expressed typical MSC surface markers, with positive staining for CD29, CD90, and CD44, and negative staining for CD34,

CD45, and CD11b (Figure 1A). These results align with established MSC identification standards. Moreover, the multilineage differentiation potential of OM-MSCs was confirmed through Alizarin Red S staining (to assess osteogenic differentiation) and Oil Red O staining (to assess adipogenic differentiation) (Figure 1B, C).

OM-MSCs-Exos were isolated from the conditioned medium of P3–P5 OM-MSCs. NTA showed that the particle size of OM-MSCs-Exos ranged from 80–180 nm, with a peak at 136 nm (Figure 1D). TEM images revealed a characteristic double-membrane spherical structure, consistent with exosome morphology (Figure 1E). Additionally, WB analysis confirmed positive expression of exosome markers CD9 and CD63 in OM-MSCs-Exos, while these markers were undetectable in OM-MSCs. Calnexin, an endoplasmic reticulum marker, was not detected in OM-MSCs-Exos (Figure 1F). Collectively, these results validated the successful isolation and characterization of OM-MSCs and OM-MSCs-Exos, meeting the established criteria for MSCs and exosomes.

3.2. OM-MSCs-Exos improve spatial learning and memory *in vivo*

To investigate the effects of OM-MSCs-Exos on cognitive function in mice with AD, behavioral experiments were conducted one month after OM-MSCs-Exos transplantation. These included the MWM and NORT to assess spatial learning and memory (Figure 2). In the NORT (Figure 2A), mice with AD that were treated with Aβ1-42 spent significantly less time exploring novel objects, indicating memory impairment induced by Aβ1-42. In contrast, OM-MSCs-Exos treatment enhanced object recognition ability compared to the AD group.

In the MWM experiment, mice with AD displayed longer escape latencies on days 4 and 5 compared to the sham and OM-MSCs-Exos groups (Figure 2B), suggesting impaired spatial learning ability in the AD group, which improved following OM-MSCs-Exos treatment. In a probe test conducted on day 7 of the spatial learning experiment, after removing the hidden platform, the number of crossings over the original platform location and the distance traveled within 90 seconds were used as indicators of spatial memory. Results showed that the OM-MSCs-Exos group traveled less distance than the AD group (Figure 2C), while the OM-MSCs-Exos group made more platform crossings compared to the AD group (Figure 2D), further substantiating the contention that OM-MSCs-Exos treatment enhances spatial memory.

Moreover, the time spent in the target quadrant (Figure 2E) was significantly longer in the OM-MSCs-Exos group than in the AD group, substantiating the cognitive improvement induced by OM-MSCs-Exos. To explore the underlying mechanism for that, ELISA was used to measure Aβ1-42 levels in hippocampal tissue (Figure

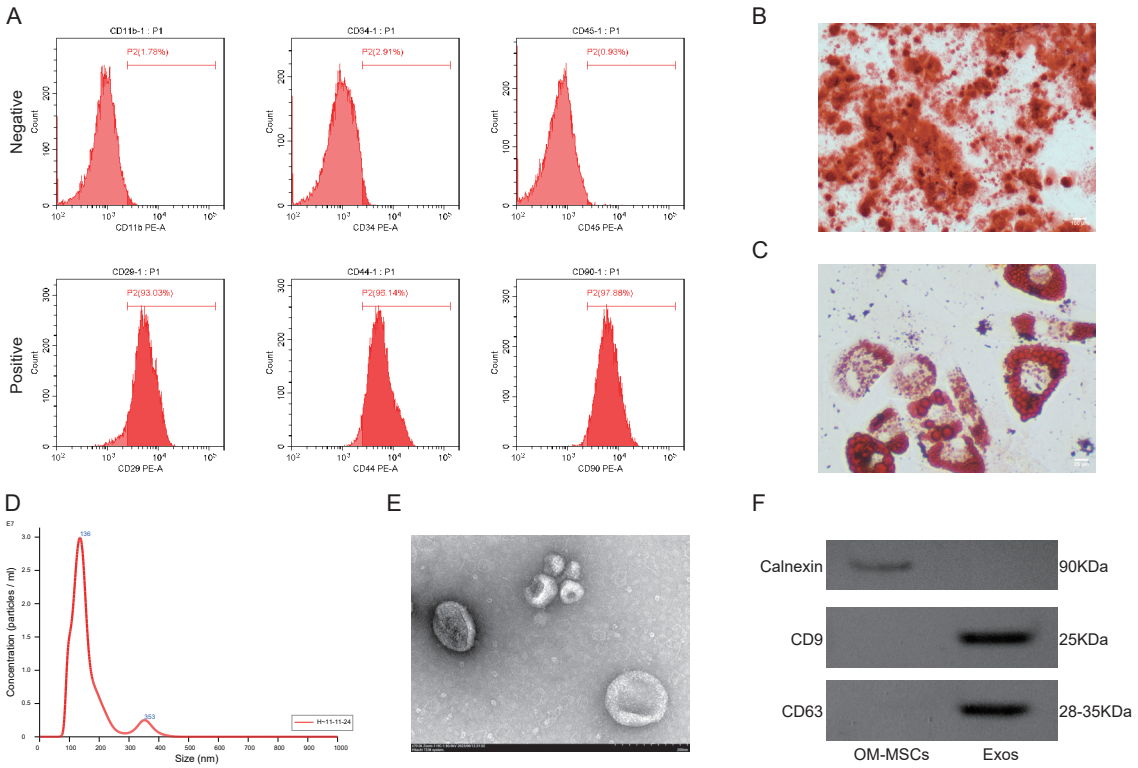

Figure 1. Characterization of OM-MSCs and OM-MSCs-Exos. (A) Flow cytometry analysis of surface markers on OM-MSCs. **(B)** Alizarin Red S staining. **(C)** Oil Red O staining. **(D)** Nanoparticle tracking analysis. **(E)** Transmission electron microscopy. **(F)** Western blot analysis of exosome marker expression.

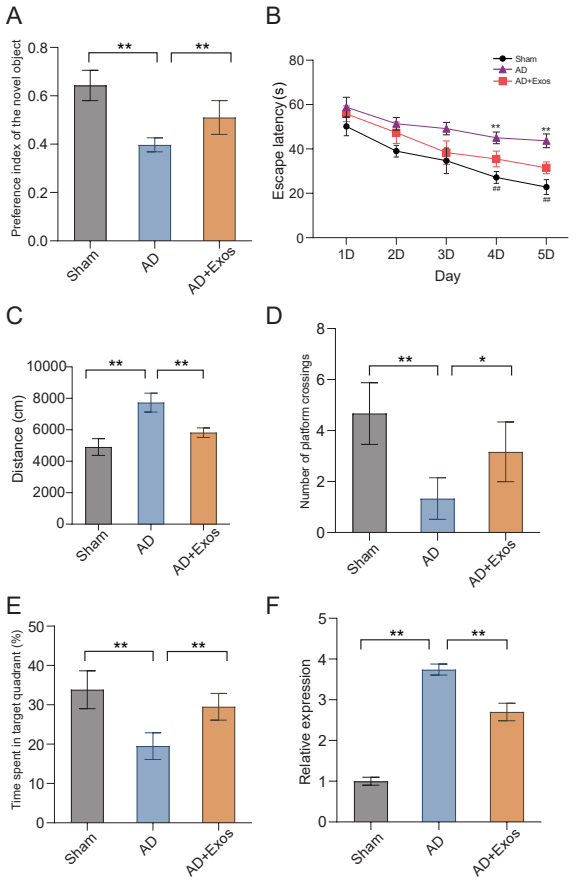

Figure 2. OM-MSCs-Exos improve spatial learning and memory in mice with AD. (A) Novel object recognition test. **(B)** Escape latency in the Morris Water Maze (MWM) (*: Sham *vs* AD; #: AD *vs* AD+Exos). **(C)** Distance traveled in the platform quadrant during the spatial exploration test. **(D)** Number of platform crossings during the spatial exploration test. **(E)** Time spent in the platform quadrant during the spatial exploration test. **(F)** ELISA analysis of changes in Aβ1-42 levels in the hippocampal tissue of mice with AD. $^{*}P < 0.05$, $^{**}P < 0.01$ and $^{\#\#}P < 0.01$.

2F). Results indicated that Aβ1-42 levels were lower in the OM-MSCs-Exos group compared to the AD group, suggesting that OM-MSCs-Exos treatment reduces Aβ1-42 deposition.

In summary, compared to mice with AD that were treated with PBS, OM-MSCs-Exos transplantation significantly improved spatial learning and memory, an effect likely associated with reduced Aβ1-42 accumulation.

3.3. OM-MSCs-Exos suppress neuroinflammation, ER stress, and neuronal loss

To examine the effects of OM-MSCs-Exos on neuroinflammation, ER stress, and neuronal loss in mice with AD, the morphology and number of Nissl bodies in brain tissue was first assessed using Nissl staining. Results revealed a significant reduction in the number and size of Nissl bodies in mice with AD. However, in mice with AD that were treated with OM-MSCs-Exos, the number of Nissl bodies markedly increased, indicating that exosomes effectively improve neuronal health (Figure 3A).

Activated microglia and astrocytes are key markers of neuroinflammation. IHC was used to detect the levels of expression of GFAP (an astrocyte marker) and Iba1 (a microglial marker) in the hippocampal region of mice with AD. Findings showed a significant increase in GFAP- and Iba1-positive cells in mice with AD. Following OM-MSCs-Exos treatment, however, the activation of these cells decreased substantially (Figure 3B-E). This suggests that OM-MSCs-Exos may mitigate neuroinflammation and protect neurons by suppressing astrocyte and microglial activation.

Next, TUNEL staining was used to detect apoptosis in mouse brain tissue. Results indicated that OM-MSCs-Exos treatment significantly reduced the number of apoptotic cells in the brains of mice with AD (Figure 3F, G). WB analysis further revealed that OM-MSCs-Exos treatment upregulated the expression of the anti-apoptotic protein Bcl-2 while downregulating the pro-apoptotic proteins Bax and cleaved caspase-3 (Figure 3H-J). These findings indicate that OM-MSCs-Exos may inhibit apoptosis *via* the Bcl-2/Bax signaling pathway, thereby reducing neuronal damage in the mouse model of AD.

To further validate the anti-inflammatory effects of OM-MSCs-Exos, ELISA was used to measure the levels of pro-inflammatory cytokines TNF-α, IL-1β, and IL-6 in the brain tissue of mice with AD. Results showed that OM-MSCs-Exos treatment significantly reduced the concentrations of these cytokines (Figure 3K), suggesting that OM-MSCs-Exos may alleviate neuroinflammation by suppressing inflammatory cytokine release.

ER stress plays a critical role in the progression of AD. WB analysis was used to assess the levels of expression of the key ER stress-related proteins CHOP, GRP78, and ATF6. Results indicated that OM-MSCs-Exos treatment downregulated the expression of GRP78, ATF6, and CHOP (Figure 3L, M). This appropriate downregulation of GRP78, ATF6, and CHOP likely contributes to alleviating neuronal damage caused by excessive ER stress.

3.4. OM-MSCs-Exos ameliorate Aβ1-42-induced ER stress, neuroinflammation, and apoptosis *in vitro*

Aβ1-42 is a key pathogenic factor in AD, and its aggregation triggers cellular stress responses, including ER stress, neuroinflammation, and apoptosis. To validate the bioactivity of OM-MSCs-Exos, their protective effects on cell viability, apoptosis, inflammation, and ER stress was further evaluated in a cellular model of AD.

First, the uptake of OM-MSCs-Exos by SH-SY5Y cells was observed using fluorescence microscopy. After co-incubating PKH67-labeled OM-MSCs-Exos with SH-SY5Y cells for 6 hours, clear green fluorescence signals

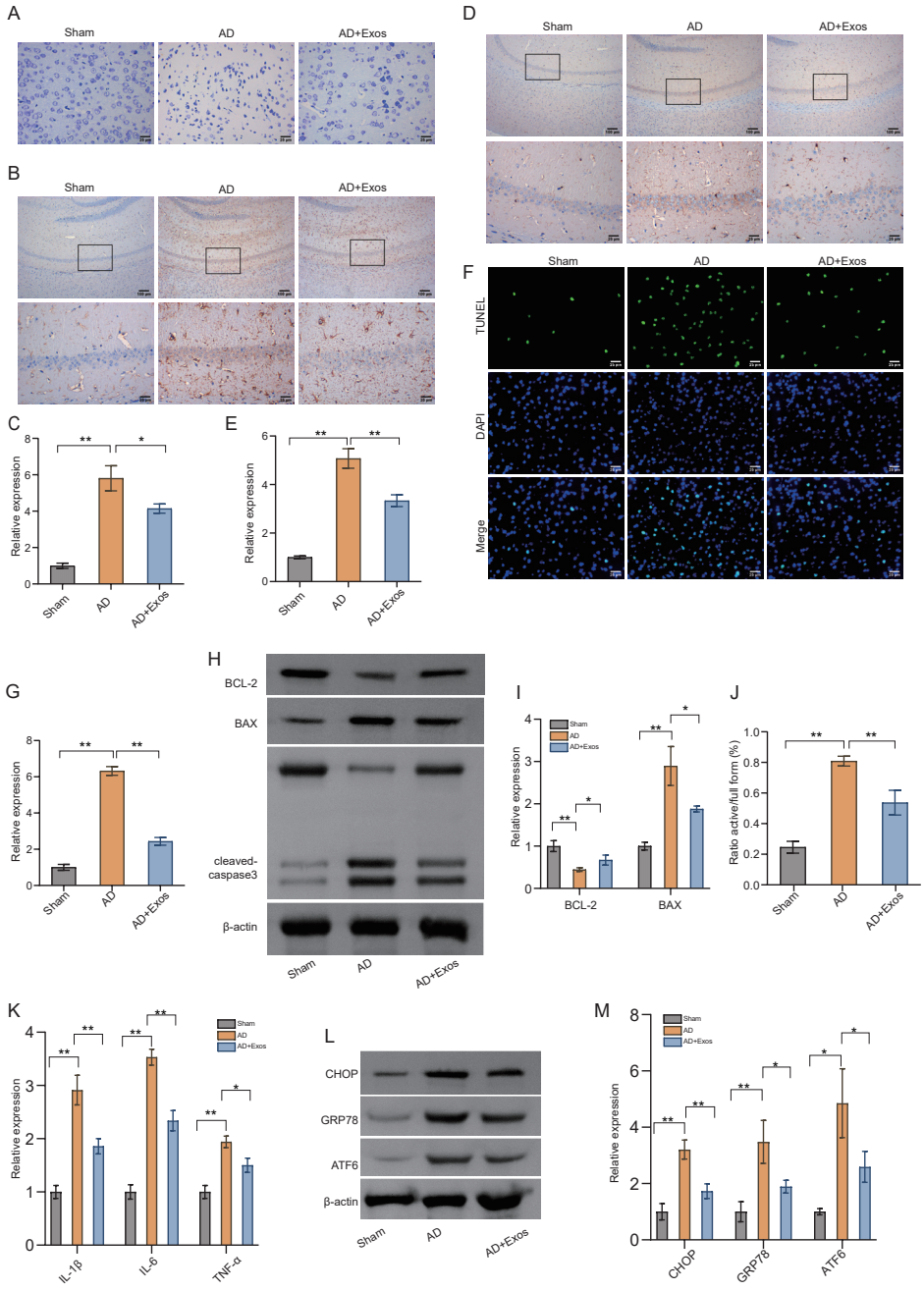

Figure 3. Neuroprotective effects of OM-MSCs-Exos in mice with AD. (A) Nissl staining of mouse brain tissue. **(B, C)** Immunohistochemical (IHC) staining and analysis of GFAP expression in the hippocampal region of mice. **(D, E)** IHC staining and analysis of Iba1 expression in the hippocampal region of mice. **(F, G)** TUNEL staining of mouse brain tissue. **(H-J)** Western blot analysis of levels of Bcl-2, Bax, and cleaved caspase-3 expression in mouse brain tissue. **(K)** ELISA analysis of TNF-α, IL-1β, and IL-6 levels in mouse brain tissue. **(L, M)** Western blot analysis of levels of CHOP, GRP78, and ATF6 expression in mouse brain tissue. $*P < 0.05$ and $**P < 0.01$.

were detected around the cell nuclei, confirming effective internalization of the exosomes (Figure 4A). Cell viability and proliferation were then assessed using the CCK-8 assay. Compared to the Aβ1-42-treated group, the OM-MSCs-Exos-treated group had significantly higher SH-SY5Y cell survival rates (Figure 4B), indicating that OM-MSCs-Exos effectively mitigate Aβ1-42-induced cell damage and promote cell survival.

To further evaluate apoptosis, Annexin V/PI dual staining flow cytometry was performed. The results showed that the total apoptosis rate in the OM-MSCs-Exos-treated group was lower than that in the Aβ1-42 group, with a notable reduction in early apoptotic cells (Figure 4C, D). WB analysis of levels of Bcl-2, Bax, and cleaved caspase-3 expression revealed that OM-MSCs-Exos treatment upregulated Bcl-2 while downregulating Bax and cleaved caspase-3 (Figure 4E-G). These findings further support the hypothesis that OM-MSCs-Exos inhibit apoptosis *via* the Bcl-2/Bax signaling pathway, exerting a neuroprotective effect.

Additionally, to investigate the suppression of Aβ1-42-induced neuroinflammatory cytokine release by OM-

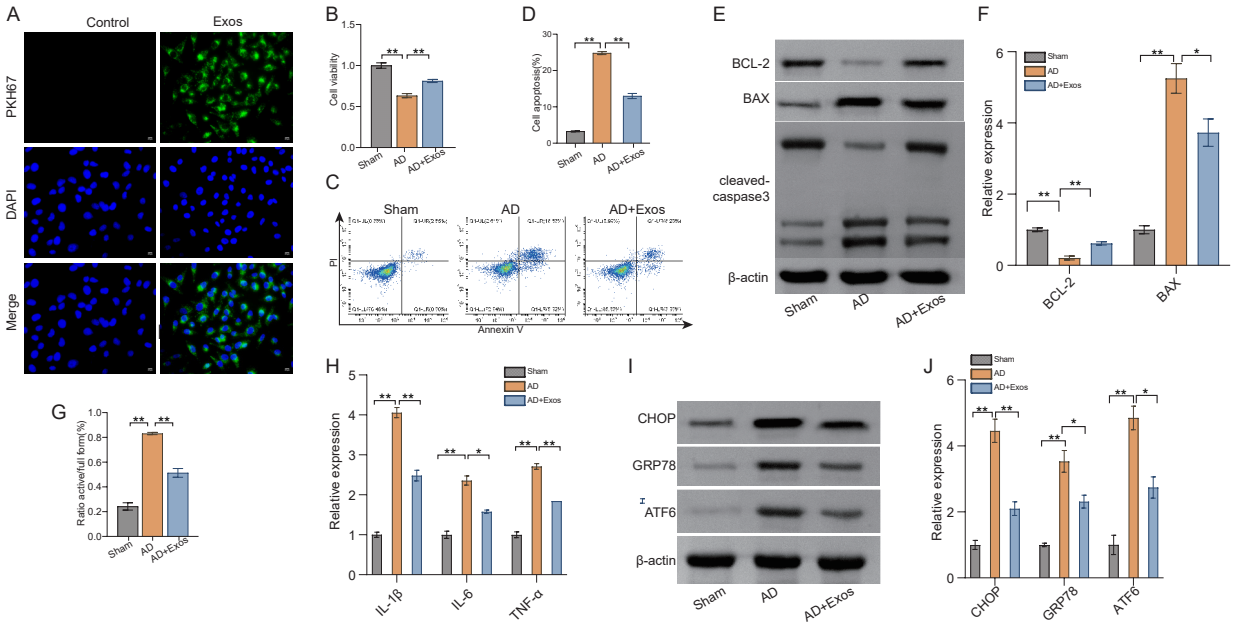

Figure 4. Neuroprotective effects of OM-MSCs-Exos in an Aβ1-42-induced SH-SY5Y cell model. (A) Fluorescence images of PKH67-labeled OM-MSCs-Exos co-cultured with SH-SY5Y cells. **(B)** CCK-8 assay to examine cell viability. **(C, D)** Annexin V/PI double staining flow cytometry to detect apoptosis. **(E-G)** Western blot analysis of Bcl-2, Bax, and cleaved caspase-3 levels. **(H)** ELISA assessment of TNF-α, IL-1β, and IL-6 levels in cell supernatant. **(I, J)** Western blot analysis of levels of CHOP, GRP78, and ATF6 expression. **P* < 0.05 and ***P* < 0.01.

MSCs-Exos, ELISA was used to measure TNF-α, IL-1β, and IL-6 levels in SH-SY5Y cell culture medium. Results indicated that OM-MSCs-Exos treatment inhibited the release of these inflammatory cytokines compared to the Aβ1-42 group (Figure 4H), indicating that OM-MSCs-Exos suppress Aβ1-42-induced neuroinflammation.

To further assess the regulation of ER stress by OM-MSCs-Exos, WB analysis was used to measure the levels of expression of the key ER stress-related proteins GRP78, ATF6, and CHOP. Results showed that OM-MSCs-Exos treatment downregulated GRP78, ATF6, and CHOP expression (Figure 4I, J). These findings suggest that OM-MSCs-Exos may alleviate Aβ1-42-induced ER stress by modulating the ER stress response, thereby protecting cells from stress-induced damage.

3.5. OM-MSCs-Exos mitigate Aβ1-42-induced ER stress, neuroinflammation, and apoptosis *via* LRP1

Although the above experiments confirmed the neuroprotective effects of OM-MSCs-Exos in models of AD, the precise molecular mechanisms remain unclear. This study further explored the role of key proteins in OM-MSCs-Exos in neuronal repair and cognitive recovery. Proteomic analysis revealed that OM-MSCs-Exos are enriched in exosome-related proteins. Xun *et al.* (*17*) identified 304 proteins secreted by OM-MSCs that are closely associated with neurotrophy, cell growth, differentiation, apoptosis, inflammation, and neuronal repair. Notably, OM-MSCs-Exos express LRP1. Previous studies have shown that LRP1 can suppress neuroinflammation and ER stress (*18-20*). Thus, the hypothesis was that OM-MSCs-Exos have a neuroprotective effect in the cellular model of AD *via* LRP1.

First, WB analysis revealed that LRP1 expression was downregulated in the cellular model of AD, while OM-MSCs-Exos treatment partially restored LRP1 expression (Figure 5A-B). These findings suggest that LRP1 may be involved in the neuroprotective effects mediated by OM-MSCs-Exos. To further validate this, LRP1 expression in OM-MSCs was silenced using siRNA, which reduced LRP1 mRNA expression in OM-MSCs-Exos (Figure 5C), confirming the efficacy of siRNA silencing. In the cellular model of AD, OM-MSCs-Exos treatment increased cell viability (Figure 5D), whereas the si-LRP1 intervention group exhibited reduced cell viability, indicating that LRP1 is linked to the neuroprotective effects of OM-MSCs-Exos. Furthermore, Annexin V/PI flow cytometry analysis showed that OM-MSCs-Exos treatment reduced apoptosis, while the si-LRP1 intervention group exhibited a significantly higher apoptosis rate (Figure 5E, F), corroborating LRP1's role in apoptosis regulation.

Additional WB analysis demonstrated that OM-MSCs-Exos treatment upregulated the anti-apoptotic protein Bcl-2 and downregulated the pro-apoptotic proteins Bax and cleaved caspase-3. However, si-LRP1 intervention reversed these protective effects, as evinced by increased Bax and cleaved caspase-3 expression and decreased Bcl-2 expression (Figure 5G-I). Moreover, ELISA results showed that OM-MSCs-Exos treatment significantly inhibited the release of the Aβ1-42-induced pro-inflammatory cytokines TNF-α, IL-1β, and IL-

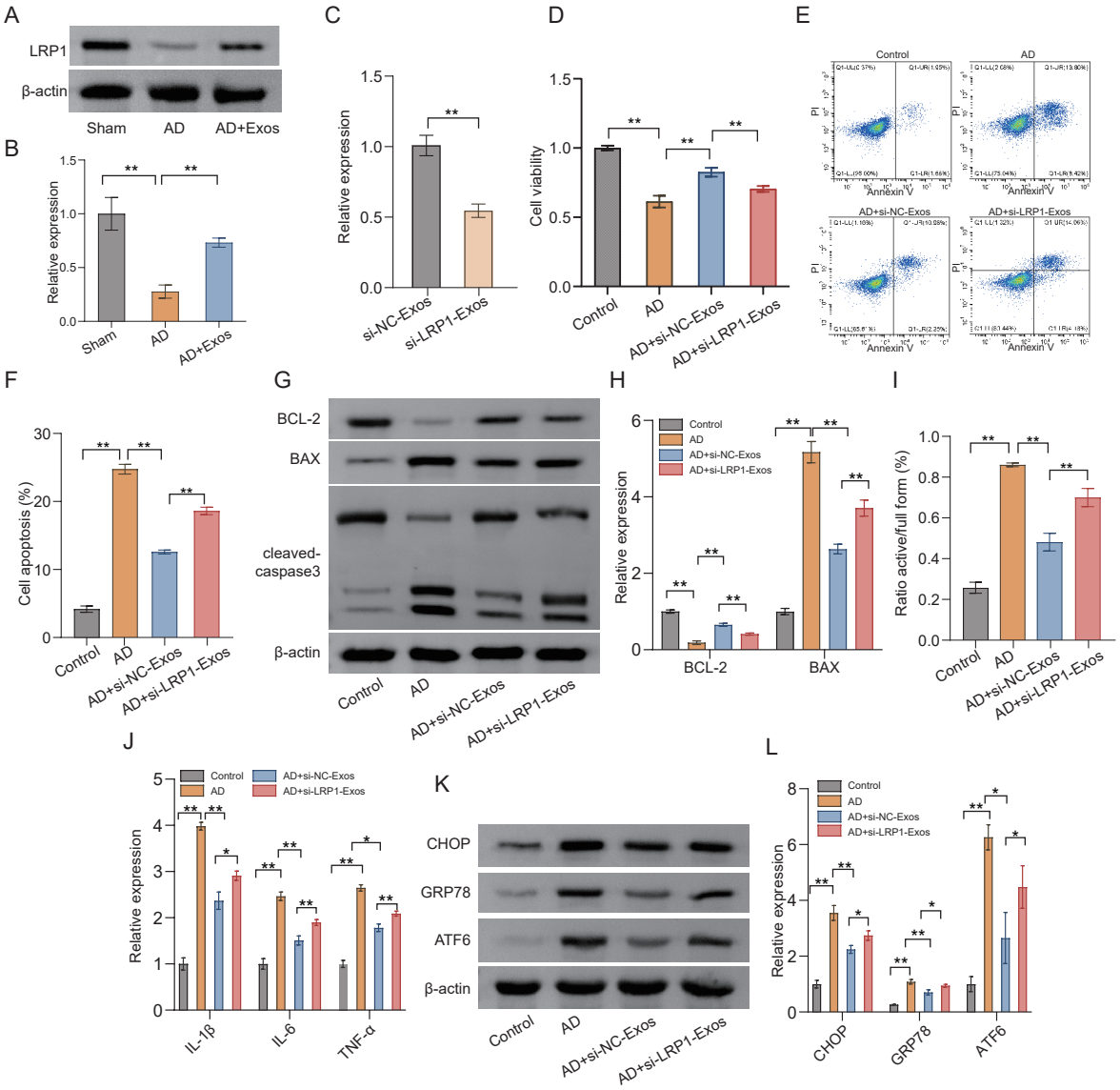

Figure 5. OM-MSCs-Exos alleviate Aβ1-42-induced SH-SY5Y cell damage by regulating LRP1 expression. (A, B) Western blot analysis of changes in LRP1 expression. **(C)** qPCR quantification of LRP1 mRNA expression. **(D)** CCK-8 assay for cell viability. **(E, F)** Annexin V/PI flow cytometry analysis of cell apoptosis. **(G-I)** Western blot analysis of levels of Bcl-2, Bax, and cleaved caspase-3 expression. **(J)** ELISA assessment of TNF-α, IL-1β, and IL-6 levels. **(K, L)** Western blot analysis of GRP78, ATF6, and CHOP expression. *$P < 0.05$ and **$P < 0.01$.

6, whereas the si-LRP1 intervention group exhibited increased cytokine release (Figure 5J).

Finally, to explore LRP1's role in ER stress, the levels of expression of the ER stress-related proteins CHOP, GRP78, and ATF6 were examined. OM-MSCs-Exos treatment downregulated GRP78, ATF6, and CHOP expression, indicating that OM-MSCs-Exos mitigate cellular damage by regulating ER stress. In contrast, the si-LRP1 intervention group showed an increased ER stress response compared to the OM-MSCs-Exos-treated group (Figure 5K, L).

3.6. Downregulation of LRP1 attenuates OM-MSCs-Exos-mediated improvements in spatial learning and memory in mice with AD

To further investigate whether LRP1 is a key molecule in OM-MSCs-Exos-mediated cognitive improvement *in vivo*, C57BL/6 mice were randomly divided into five groups: a sham group, an AD group, an AD+OM-MSCs-Exos group, an AD+si-NC-Exos group, and an AD+si-LRP1-Exos group. After 4 weeks of treatment, cognitive behavioral tests, including the NORT and MWM, were performed (Figure 6A-E).

In the NORT, mice with AD spent less time exploring novel objects, indicating memory impairment due to Aβ1-42 treatment. OM-MSCs-Exos treatment enhanced object recognition ability compared to the AD group. However, the si-LRP1-Exos group spent less time exploring, suggesting that LRP1 suppression diminished the memory-enhancing effects of OM-MSCs-Exos (Figure 6A).

In the MWM test, differences in escape latency were observed on days 4 and 5. Compared to the AD

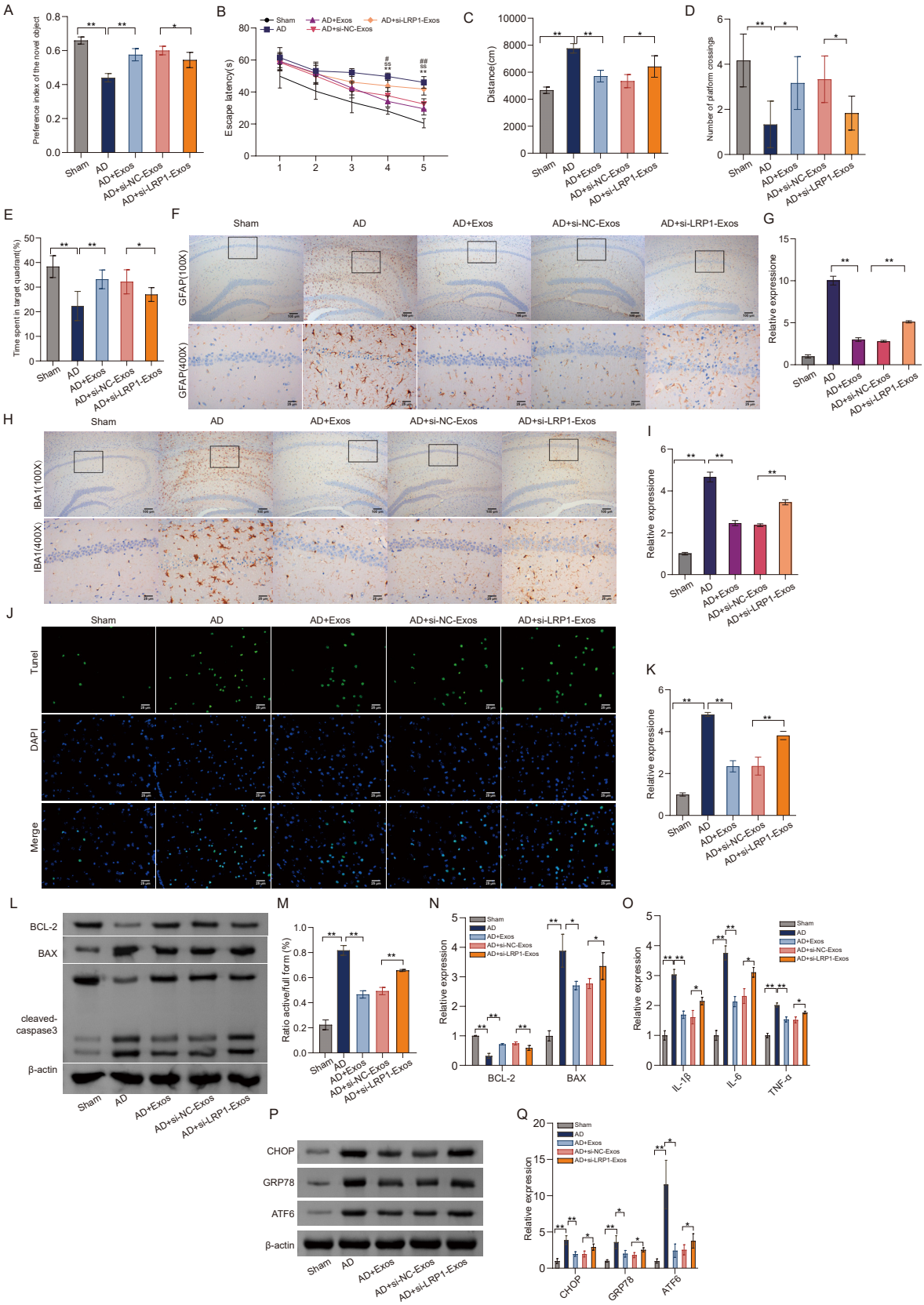

Figure 6. Downregulation of LRP1 attenuates the cognitive enhancement brought about by OM-MSCs-Exos in mice with AD. (A) Novel object recognition test. **(B)** Escape latency in the MWM (*: Sham *vs* AD; #: AD *vs* AD+Exos; s:AD+si-NC-Exos *vs* AD+si-LRP1-Exos). **(C)** Distance traveled in the platform quadrant during the spatial exploration test. **(D)** Number of platform crossings during the spatial exploration test. **(E)** Time spent in the platform quadrant during the spatial exploration test. **(F, G)** IHC analysis of GFAP expression in the hippocampal region of mice. **(H, I)** IHC analysis of Iba1 expression in the hippocampal region of mice. **(J, K)** TUNEL detection of apoptosis in brain tissue. **(L-N)** Western blot analysis of Bcl-2, Bax, and cleaved caspase-3 expression. **(O)** ELISA analysis of TNF-α, IL-1β, and IL-6 levels in mouse brain tissue. **(P-Q)** Western blot analysis of GRP78, ATF6, and CHOP expression in mouse brain tissue. $^{*}P < 0.05$, $^{**}P < 0.01$, $^{\#}P < 0.01$, $^{\#\#}P < 0.05$, and $^{ss}P < 0.01$.

group, OM-MSCs-Exos-treated mice had shorter escape latencies, indicating improved spatial learning ability. However, the si-LRP1-Exos group had slightly longer escape latencies, suggesting that LRP1 suppression diminished the ability of OM-MSCs-Exos to enhance spatial learning (Figure 6B). The number of crossings over the original platform location (Figure 6D) and distance traveled (Figure 6C) within 90 seconds revealed that the OM-MSCs-Exos group crossed the platform more frequently and traveled less distance than the AD group, confirming the efficacy of OM-MSCs-Exos in enhancing spatial memory. In contrast, the si-LRP1-Exos group made fewer crossings and traveled a longer distance compared to the si-NC-Exos group, indicating that LRP1 suppression attenuated the spatial memory improvements mediated by OM-MSCs-Exos.

Furthermore, OM-MSCs-Exos-treated mice spent more time in the target quadrant than the AD group, reflecting enhanced spatial memory and target recognition ability. Compared to the si-NC-Exos group, the si-LRP1-Exos group spent less time in the target quadrant, further corroborating the critical role of LRP1 in OM-MSCs-Exos-mediated cognitive protection (Figure 6E).

3.7. Downregulation of LRP1 attenuates the effects of OM-MSCs-Exos on cognitive improvement and amelioration of ER stress, neuroinflammation, and apoptosis *in vivo*

To investigate the neuroprotective role of LRP1 in AD pathogenesis, IHC was used to analyze the levels of expression of the microglial marker Iba1 and the astrocytic marker GFAP in the hippocampal tissue of mice with AD (Figure 6F-I). Results showed that the OM-MSCs-Exos group had significantly reduced Iba1 and GFAP expression compared to the AD group, indicating that OM-MSCs-Exos effectively suppress neuroinflammatory responses. However, Iba1 and GFAP expression increased in the si-LRP1-Exos group compared to the si-NC-Exos group, suggesting that LRP1 suppression diminished the anti-inflammatory effects of OM-MSCs-Exos.

TUNEL staining was used to detect apoptosis in mouse brain tissue (Figure 6J, K). Results revealed that the OM-MSCs-Exos group had significantly fewer apoptotic cells than the AD group, indicating that OM-MSCs-Exos effectively inhibit neuronal apoptosis in mice with AD. However, the number of apoptotic cells increased significantly in the si-LRP1-Exos group compared to the si-NC-Exos group, further demonstrating that LRP1 suppression diminished the neuroprotective effects of OM-MSCs-Exos.

To further evaluate changes in the apoptosis signaling pathway, WB analysis was performed to assess the levels of Bcl-2, Bax, and cleaved caspase-3 expression. Compared to the AD group, the OM-MSCs-Exos group displayed upregulated Bcl-2 expression and downregulated Bax and cleaved caspase-3 expression, indicating that OM-MSCs-Exos effectively suppress the activation of the apoptosis signaling pathway (Figure 6L-N). However, levels of Bax and cleaved caspase-3 expression significantly increased in the si-LRP1-Exos group while Bcl-2 expression decreased. These findings further suggest that LRP1 suppression diminishes the inhibitory effect of OM-MSCs-Exos on the apoptosis signaling pathway.

ELISA was used to measure the levels of pro-inflammatory cytokines TNF-α, IL-1β, and IL-6 in mouse brain tissue. Results showed that the OM-MSCs-Exos group had significantly lower levels of these cytokines compared to the AD group (Figure 6O), indicating that OM-MSCs-Exos effectively suppress inflammation. However, the levels of these inflammatory cytokines increased in the si-LRP1-Exos group compared to the OM-MSCs-Exos group, further demonstrating that LRP1 suppression diminished the anti-inflammatory effects of exosomes.

Finally, to investigate changes in ER stress, WB analysis was used to assess the levels of expression of the ER stress-related proteins CHOP, GRP78, and ATF6. The OM-MSCs-Exos group had significantly reduced CHOP, GRP78, and ATF6 expression compared to the AD group (Figure 6P, Q), indicating that OM-MSCs-Exos effectively alleviate ER stress in mice with AD. However, levels of CHOP, GRP78, and ATF6 expression increased again in the si-LRP1-Exos group, suggesting that LRP1 suppression diminished the protective effects of OM-MSCs-Exos on ER stress alleviation.

4. Discussion

AD is a complex neurodegenerative disorder typically characterized by a progressive decline in cognitive function and neuronal dysfunction (*21*). The pathological progression of AD is driven by multiple factors, with neuroinflammation and ER stress being considered key contributors (*22,23*). The hallmark pathological features of AD are the deposition of Aβ and the abnormal phosphorylation of tau protein. These aberrant changes not only directly impair neurons but also exacerbate disease progression by triggering neuroinflammatory responses (*24*). In the brains of patients with AD, persistent low-level neuroinflammation is commonly observed, with the activation of microglia and astrocytes being considered the primary sources of inflammation (*25*). Elevated levels of pro-inflammatory cytokines, such as TNF-α, IL-6, and IL-1β, contribute to neuronal damage and dysfunction, thereby promoting neurodegeneration (*26*).

ER stress also plays an important role in the pathological development of AD (*27*). When misfolded proteins accumulate in the ER, the unfolded protein response (UPR) is activated to restore ER homeostasis.

However, prolonged or severe ER stress can trigger pro-apoptotic signaling pathways, particularly in neurons, making it a significant contributor to cell death in AD (*28*). Aβ deposition is recognized as a key inducer of ER stress, disrupting ER function and thereby amplifying neuronal damage (*29*). In the current study, levels of the pro-inflammatory cytokines IL-1β, IL-6, and TNF-α were significantly elevated in a mouse model of AD, and ER-associated proteins such as CHOP, GRP78, and ATF6 were markedly upregulated. Immunofluorescence staining further revealed a significant increase in the activation of Iba1-positive microglia and GFAP-positive astrocytes in the hippocampal region. These findings suggest that suppressing neuroinflammation and excessive ER stress may offer potential benefits in terms of alleviating AD-related neurological deficits.

In recent years, MSCs have shown considerable promise in the treatment of various neurodegenerative diseases (*30*). Traditionally, MSCs are derived from mesodermal tissues such as bone marrow and adipose tissue. These MSCs display some neuroprotective effects in terms of neural repair, but there are several with their clinical use, including limited neurogenic differentiation potential, ethical concerns, and difficulties in crossing the BBB (*31*). In contrast, OM-MSCs, which originate from ectodermal tissue, demonstrate greater neurogenic differentiation potential, positioning them as a more promising candidate for neural repair. Moreover, OM-MSCs can be isolated from human nasal mucosa *via* minimally invasive procedures, offering excellent biosafety and circumventing the ethical controversies associated with other stem cell sources. However, there are obstacles to the direct transplantation of OM-MSCs, such as challenges in crossing the BBB and potential tumorigenic risks. Unlike stem cells, exosomes derived from stem cells cannot self-replicate, eliminating the risk of tumor formation associated with stem cell transplantation (*21*). Consequently, exosomes have emerged as a safer and more effective therapeutic strategy. Exosomes are vesicles enclosed by a lipid bilayer, distinguished by the presence of tetraspanins (CD9, CD81, and CD63), ALG-2-interacting protein X (Alix), and tumor susceptibility gene 101 protein (TSG101) on their membrane surface (*32*). They can carry a variety of bioactive molecules, including proteins, nucleic acids, and lipids, and are capable of crossing the BBB to deliver therapeutic agents, making them a focal point in research on neurodegenerative diseases such as AD, stroke, and traumatic brain injury (*33,34*).

The current study successfully isolated and characterized OM-MSCs-Exos. TEM, NTA, and WB confirmed that these exosomes exhibit a typical lipid bilayer structure and express exosome markers. Further immunofluorescence staining demonstrated that PKH67-labeled OM-MSCs-Exos were effectively internalized by cells. These results indicate that OM-MSCs-Exos significantly inhibited the activation of microglia and astrocytes in the hippocampus, reduced the release of pro-inflammatory cytokines in brain tissue, and lowered the levels of expression of ER stress-related proteins. These effects were closely associated with significant improvements in cognitive function and reduced neuronal apoptosis in mice with AD. Conventional ultracentrifugation was used during the isolation of OM-MSCs-Exos. However, the purity and yield of exosomes may be influenced by factors such as cell culture conditions and centrifugation parameters, which could potentially interfere with subsequent results (*35,36*). Moreover, fluorescence labeling experiments have demonstrated that OM-MSCs-Exos can be taken up by cells, but their specific sites of action and underlying mechanisms within the cells remain unclear. To address this, more in-depth studies, possibly utilizing techniques such as confocal microscopy, may need to be conducted.

To further elucidate the neuroprotective mechanisms of OM-MSCs-Exos, the proteomic profile of OM-MSCs-Exos as reported by Xun *et al.* (*17*) was analyzed, and enrichment of LRP1 in these exosomes was noted. Previous studies have demonstrated that LRP1 plays a critical role in regulating the activation of microglia and astrocytes as well as modulating inflammatory responses (*18,37,38*). Additionally, LRP1 influences ER stress-related signaling pathways, impacting cell survival and function (*39*). The current findings revealed that LRP1 expression decreased significantly in a mouse model of AD, while ER stress and pro-inflammatory cytokine levels increased markedly. Following OM-MSCs-Exos treatment, however, LRP1 expression in mouse brain tissue increased, accompanied by an alleviation of both ER stress and inflammatory responses. Further experiments that used siRNA to silence LRP1 expression in OM-MSCs demonstrated that the neuroprotective effects of OM-MSCs-Exos in suppressing ER stress and neuroinflammation significantly diminished, underscoring the central role of LRP1 in the neuroprotective mechanisms of OM-MSCs-Exos treatment. However, the pathogenesis of AD is highly complex, involving the interplay of multiple cell types and signaling pathways (*40*). In addition to the known mechanisms, OM-MSCs-Exos may have an effect through other as yet unidentified pathways.

From a clinical translation perspective, the long-term stability, dose-dependency, and immunogenicity of exosomes warrant further evaluation. Although this study has demonstrated that OM-MSCs-Exos improve cognitive function in AD, their therapeutic efficacy across different stages of AD remains unclear. Future research could utilize multi-omics approaches, such as single-cell transcriptomics and protein interactomics, to further clarify the mechanisms of OM-MSCs-Exos and optimize their therapeutic potential through pharmacological enhancement.

5. Conclusion

This study provides the first evidence that OM-MSCs-Exos can significantly enhance cognitive function in mice with AD. The neuroprotective effects of OM-MSCs-Exos appear to be mediated through the suppression of neuroinflammatory responses, attenuation of microglial and astrocytic activation, and reduction in the expression of pro-inflammatory cytokines and ER stress markers, thereby mitigating neuronal damage. Furthermore, LRP1 may play a key role in these protective mechanisms. These findings provide novel insights into the molecular pathways underlying the therapeutic potential of OM-MSCs-Exos in the treatment of AD. However, despite these promising results, further research is required to evaluate the long-term stability, dose dependency, and immunogenicity of OM-MSCs-Exos, as well as to validate their clinical applicability and safety.

Acknowledgements

The authors sincerely thank Professor Wei Tang (University of Tokyo, Japan) and Professor Peipei Song (National Center for Global Health and Medicine, Japan) for their invaluable guidance and insightful discussions, which have significantly contributed to the study.

Funding: This work was supported by grants from National Natural Science Foundation of China (82460268), the Hainan Province Clinical Medical Research Center (No. LCYX202410, LCYX202309), and the Hainan Province Postdoctoral Research Project (403254).

Conflict of Interest: The authors have no conflicts of interest to disclose.

References

1. Scheltens P, De Strooper B, Kivipelto M, Holstege H, Chetelat G, Teunissen CE, Cummings J, van der Flier WM. Alzheimer's disease. Lancet. 2021; 397:1577-1590.
2. Botella Lucena P, Heneka MT. Inflammatory aspects of Alzheimer's disease. Acta Neuropathol. 2024; 148:31.
3. Lee JH, Won SM, Suh J, Son SJ, Moon GJ, Park UJ, Gwag BJ. Induction of the unfolded protein response and cell death pathway in Alzheimer's disease, but not in aged Tg2576 mice. Exp Mol Med. 2010; 42:386-394.
4. Unterberger U, Hoftberger R, Gelpi E, Flicker H, Budka H, Voigtlander T. Endoplasmic reticulum stress features are prominent in Alzheimer disease but not in prion diseases *in vivo*. J Neuropathol Exp Neurol. 2006; 65:348-357.
5. Hoozemans JJ, van Haastert ES, Nijholt DA, Rozemuller AJ, Eikelenboom P, Scheper W. The unfolded protein response is activated in pretangle neurons in Alzheimer's disease hippocampus. Am J Pathol. 2009; 174:1241-1251.
6. Ajoolabady A, Lindholm D, Ren J, Pratico D. ER stress and UPR in Alzheimer's disease: Mechanisms, pathogenesis, treatments. Cell Death Dis. 2022; 13:706.
7. Chiti F, Dobson CM. Protein misfolding, Amyloid formation, and human disease: A summary of progress over the last decade. Annu Rev Biochem. 2017; 86:27-68.
8. Andrzejewska A, Dabrowska S, Lukomska B, Janowski M. Mesenchymal stem cells for neurological disorders. Adv Sci (Weinh). 2021; 8:2002944.
9. Liu S, Fan M, Xu JX, Yang LJ, Qi CC, Xia QR, Ge JF. Exosomes derived from bone-marrow mesenchymal stem cells alleviate cognitive decline in AD-like mice by improving BDNF-related neuropathology. J Neuroinflammation. 2022; 19:35.
10. Lin F, Chen W, Zhou J, Zhu J, Yao Q, Feng B, Feng X, Shi X, Pan Q, Yu J, Li L, Cao H. Mesenchymal stem cells protect against ferroptosis *via* exosome-mediated stabilization of SLC7A11 in acute liver injury. Cell Death Dis. 2022; 13:271.
11. Guo M, Yin Z, Chen F, Lei P. Mesenchymal stem cell-derived exosome: A promising alternative in the therapy of Alzheimer's disease. Alzheimers Res Ther. 2020; 12:109.
12. Tian J, Zhu Q, Zhang Y, Bian Q, Hong Y, Shen Z, Xu H, Rui K, Yin K, Wang S. Olfactory ecto-mesenchymal stem cell-derived exosomes ameliorate experimental colitis *via* modulating Th1/Th17 and Treg cell responses. Front Immunol. 2020; 11:598322.
13. Care IoLARCo, Animals UoL. Guide for the care and use of laboratory animals. US Department of Health and Human Services, Public Health Service, National Institutes of Health, 1986.
14. Yu L, Wang S, Chen X, Yang H, Li X, Xu Y, Zhu X. Orientin alleviates cognitive deficits and oxidative stress in Abeta1-42-induced mouse model of Alzheimer's disease. Life Sci. 2015; 121:104-109.
15. Xu M, Huang H, Mo X, Zhu Y, Chen X, Li X, Peng X, Xu Z, Chen L, Rong S, Yang W, Liu S, Liu L. Quercetin-3-O-Glucuronide alleviates cognitive deficit and toxicity in Abeta(1-42)-induced AD-like mice and SH-SY5Y cells. Mol Nutr Food Res. 2021; 65:e2000660.
16. Chen HX, Liang FC, Gu P, Xu BL, Xu HJ, Wang WT, Hou JY, Xie DX, Chai XQ, An SJ. Exosomes derived from mesenchymal stem cells repair a Parkinson's disease model by inducing autophagy. Cell Death Dis. 2020; 11:288.
17. Xun C, Ge L, Tang F, Wang L, Zhuo Y, Long L, Qi J, Hu L, Duan D, Chen P, Lu M. Insight into the proteomic profiling of exosomes secreted by human OM-MSCs reveals a new potential therapy. Biomed Pharmacother. 2020; 131:110584.
18. Yang L, Liu CC, Zheng H, Kanekiyo T, Atagi Y, Jia L, Wang D, N'Songo A, Can D, Xu H, Chen XF, Bu G. LRP1 modulates the microglial immune response *via* regulation of JNK and NF-kappaB signaling pathways. J Neuroinflammation. 2016; 13:304.
19. Mantuano E, Henry K, Yamauchi T, Hiramatsu N, Yamauchi K, Orita S, Takahashi K, Lin JH, Gonias SL, Campana WM. The unfolded protein response is a major mechanism by which LRP1 regulates Schwann cell survival after injury. J Neurosci. 2011; 31:13376-13385.
20. Hamlin AN, Basford JE, Jaeschke A, Hui DY. LRP1 protein deficiency exacerbates palmitate-induced steatosis and toxicity in hepatocytes. J Biol Chem. 2016; 291:16610-16619.
21. Ma YN, Hu X, Karako K, Song P, Tang W, Xia Y. Exploring the multiple therapeutic mechanisms and challenges of mesenchymal stem cell-derived exosomes in Alzheimer's disease. Biosci Trends. 2024; 18:413-430.

22. Nagar P, Sharma P, Dhapola R, Kumari S, Medhi B, HariKrishnaReddy D. Endoplasmic reticulum stress in Alzheimer's disease: Molecular mechanisms and therapeutic prospects. Life Sci. 2023; 330:121983.
23. Santos LE, Ferreira ST. Crosstalk between endoplasmic reticulum stress and brain inflammation in Alzheimer's disease. Neuropharmacol. 2018; 136:350-360.
24. Leng F, Edison P. Neuroinflammation and microglial activation in Alzheimer disease: Where do we go from here? Nat Rev Neurol. 2021; 17:157-172.
25. Hu X, Ma YN, Xia Y. Association between abnormal lipid metabolism and Alzheimer's disease: New research has revealed significant findings on the APOE4 genotype in microglia. Biosci Trends. 2024; 18:195-197.
26. Firdous SM, Khan SA, Maity A. Oxidative stress-mediated neuroinflammation in Alzheimer's disease. Naunyn Schmiedebergs Arch Pharmacol. 2024; 397:8189-8209.
27. Singh R, Kaur N, Choubey V, Dhingra N, Kaur T. Endoplasmic reticulum stress and its role in various neurodegenerative diseases. Brain Res. 2024; 1826:148742.
28. Lim D, Tapella L, Dematteis G, Genazzani AA, Corazzari M, Verkhratsky A. The endoplasmic reticulum stress and unfolded protein response in Alzheimer's disease: A calcium dyshomeostasis perspective. Ageing Res Rev. 2023; 87:101914.
29. Ekundayo BE, Obafemi TO, Adewale OB, Obafemi BA, Oyinloye BE, Ekundayo SK. Oxidative stress, endoplasmic reticulum stress and apoptosis in the pathology of Alzheimer's disease. Cell Biochem Biophys. 2024; 82:457-477.
30. Giovannelli L, Bari E, Jommi C, Tartara F, Armocida D, Garbossa D, Cofano F, Torre ML, Segale L. Mesenchymal stem cell secretome and extracellular vesicles for neurodegenerative diseases: Risk-benefit profile and next steps for the market access. Bioact Mater. 2023; 29:16-35.
31. Rahimi Darehbagh R, Seyedoshohadaei SA, Ramezani R, Rezaei N. Stem cell therapies for neurological disorders: Current progress, challenges, and future perspectives. Eur J Med Res. 2024; 29:386.
32. Kalluri R, LeBleu VS. The biology, function, and biomedical applications of exosomes. science. 2020; 367:eaau6977.
33. Mot YY, Moses EJ, Mohd Yusoff N, Ling KH, Yong YK, Tan JJ. Mesenchymal stromal cells-derived exosome and the roles in the treatment of traumatic brain injury. Cell Mol Neurobiol. 2023; 43:469-489.
34. Pratiwi DIN, Alhajlah S, Alawadi A, Hjazi A, Alawsi T, Almalki SG, Alsalamy A, Kumar A. Mesenchymal stem cells and their extracellular vesicles as emerging therapeutic tools in the treatment of ischemic stroke. Tissue Cell. 2024; 87:102320.
35. Xu K, Jin Y, Li Y, Huang Y, Zhao R. Recent progress of exosome isolation and peptide recognition-guided strategies for exosome research. Front Chem. 2022; 10:844124.
36. Yang D, Zhang W, Zhang H, Zhang F, Chen L, Ma L, Larcher LM, Chen S, Liu N, Zhao Q, Tran PHL, Chen C, Veedu RN, Wang T. Progress, opportunity, and perspective on exosome isolation - Efforts for efficient exosome-based theranostics. Theranostics. 2020; 10:3684-3707.
37. He Y, Ruganzu JB, Jin H, Peng X, Ji S, Ma Y, Zheng L, Yang W. LRP1 knockdown aggravates Abeta(1-42)-stimulated microglial and astrocytic neuroinflammatory responses by modulating TLR4/NF-kappaB/MAPKs signaling pathways. Exp Cell Res. 2020; 394:112166.
38. He Y, Ruganzu JB, Zheng Q, Wu X, Jin H, Peng X, Ding B, Lin C, Ji S, Ma Y, Yang W. Silencing of LRP1 exacerbates inflammatory response *via* TLR4/NF-kappaB/MAPKs signaling pathways in APP/PS1 transgenic mice. Mol Neurobiol. 2020; 57:3727-3743.
39. Wan C, Liu XQ, Chen M, Ma HH, Wu GL, Qiao LJ, Cai YF, Zhang SJ. Tanshinone IIA ameliorates Abeta transendothelial transportation through SIRT1-mediated endoplasmic reticulum stress. J Transl Med. 2023; 21:34.
40. Monteiro AR, Barbosa DJ, Remiao F, Silva R. Alzheimer's disease: Insights and new prospects in disease pathophysiology, biomarkers and disease-modifying drugs. Biochem Pharmacol. 2023; 211:115522.

Received February 8, 2025; Revised March 3, 2025; Accepted March 16, 2025.

Address correspondence to:
Ying Xia, Department of Neurosurgery, Haikou Affiliated Hospital of Central South University Xiangya School of Medicine, Haikou 570208, China.
E-mail: xiaying008@163.com

Released online in J-STAGE as advance publication March 18, 2025.